

# Analysis of ZnO varistors prepared from high-energy mechanical activation

W. J. Cai · G. R. Li · Q. R. Yin

Published online: 23 May 2007  
© Springer Science + Business Media, LLC 2007

**Abstract** ZnO varistors were prepared by high-energy mechanical activation to study its effect on the microstructure and electrical properties. Comparison of different permutation and combination of ZnO powders and additives subjected to activation for 0, 6 and 12 h were given in  $I$ – $V$ ,  $C$ – $V$ , complex resistance study. The variation of Schottky barrier height  $\Phi_b$ , donor concentration  $N_d$ , interface state density  $N_t$  and depletion layer width  $L$  were calculated in different samples. Finally, individual grain boundaries were investigated by SSPM (Scanning Surface Potential Microscopy) under in situ applied fields, allowing determination of the voltage dependence of grain boundary electronic properties.

**Keyword** ZnO Varistors · High-energy mechanical activation · Scanning Surface Potential Microscopy (SSPM) · Kelvin Force Microscopy (KFM)

## 1 Introduction

Capability of protecting circuits from overvoltages repeatedly without being destroyed is genuinely prerequisite for a well qualified varistor. It has been reported that inhomogeneous microstructures in varistors often suffer from a great spread in the current/voltage characteristics due to high local currents and overload caused by single large grains,

which gives rise to rapid degradation of varistors in electrical operation. There was a report [1] on preparing ZnO varistors using high-energy mechanical activation in small quantity for laboratory purpose. However, their micro properties accounting for the macro electronic properties of varistors were left to be investigated systematically.

In present case, we mainly concern on twofold: (1) to improve the homogeneity of the sintering precursors in large quantity (10 kg a time for industry purpose) which leads to the improved homogeneity of the mixed oxide composition; and (2) to investigate the effects of high-energy mechanical activation on the macro electrical properties such as nonlinear coefficient, breakdown voltage correlated to micro properties such as Schottky barrier height, depletion width and grain boundary resistance.

## 2 Experimental procedure

The composition of 95.6 mol% ZnO (>99.0% purity), 4.4 mol% additive powders composed of chemical pure  $Sb_2O_3$ ,  $Bi_2O_3$ ,  $Co_3O_4$ ,  $Cr_2O_3$  and MnO was used as starting material. The commercially available ZnO powder and the additives were separately ground by high-energy mechanical activation at the speed of 1,000 rpm using zirconia balls of 0.8 mm in diameter in distilled water.

Permutation and combination of ZnO powder and additive with different activation time was made as follows: 0 h activated ZnO powder with 0 h activated additive, 6 h activated ZnO powder with 6 h activated additive, 6 h activated ZnO powder with 12 h activated additive, 12 h activated ZnO powder with 6 h activated additive, 12 h activated ZnO powder with 12 h activated additive, batches were abbreviated as A, B, C, D, E. These powders were mixed by planetary ball milling in

---

W. J. Cai (✉) · G. R. Li · Q. R. Yin  
State Key Laboratory of High Performance Ceramics and Superfine Structures, Shanghai Institute of Ceramics, Chinese Academy of Sciences, Shanghai 200050, People's Republic of China  
e-mail: wjcai@mail.sic.ac.cn

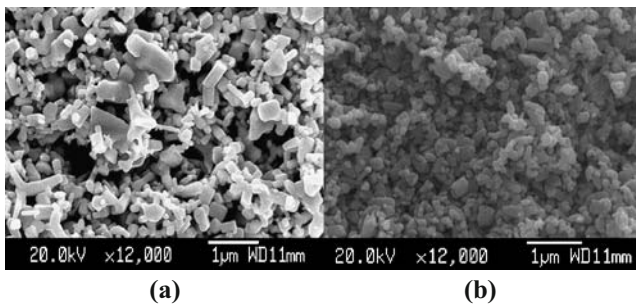


**Fig. 1** SEM photos of the Zinc oxide powder subjected to (a) 0 h, (b) 12 h activation

a polyethylene jar containing various size of zirconia milling balls from 2 to 5 mm in diameter at the speed of 406 rpm for 6 h.

The five kinds of powders were then uniaxially compacted in a steel die of 20 mm in diameter at the pressure of 1.5 MPa. Sintering was conducted at 1140 °C for 2 h at the rate of 5 °C/min. The opposite sides were coated with silver paint for electrical measurement.

Scanning Electron Microscope (JEOL, JSM-6700F) is used for observation of powder and for polished and thermally etched disk section, respectively. Average grain size  $d$  was obtained using classical intercept method. Their specific surface areas were measured using a BET surface analyzer (Micromeritics, Tristar-3000). Densification was studied with linear shrinkage at constant heating rate of 5 °C/min using DIL 402-E (Netzsch, Germany) while the density was measured by the Archimedes method. The impedance and capacitance measurements were conducted at 190 °C and room temperature using a Hewlett-Packard 4294A Impedance Analyzer. The frequency was from 40 Hz to 10 MHz for complex resistance measurement. Capacitance was obtained with the bias voltage ranging from 0–40 V superimposing on an AC signal of 10 kHz frequency. The scanning surface potential microscopy (SSPM) was studied using commercial Atomic Force

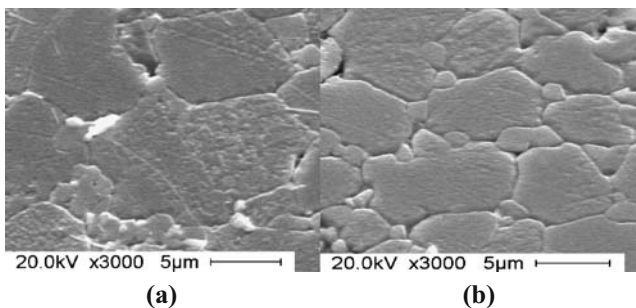


**Fig. 2** SEM micrographs of thermally etched surface of pellets (a) Sample A, (b) Sample E sintered at 1140 °C for 2 h

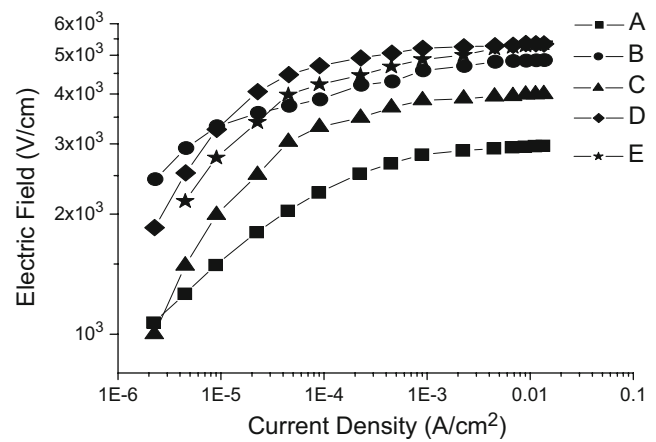


**Fig. 3**  $I$ - $V$  characteristics of Sample A to E sintered at 1140 °C

Microscope (SPI3800N & SPA300HV, Seiko Instrument Inc., Japan) with Kelvin Force Probe at the lift height 60 nm and with the  $\pm 1$  V lateral bias voltage.

Breakdown voltage ( $V_{bk}$ ) was determined on  $I$ - $V$  curve at the current density of 1 mA/cm<sup>2</sup>. Leakage current ( $I_L$ ) was read on 0.75  $V_{bk}$ . Nonlinear coefficient ( $\alpha$ ) was calculated as  $\alpha = \log(I_2/I_1) / \log(V_2/V_1)$  using the voltages at 1.0 and 10 mA/cm<sup>2</sup>. Capacitances ( $C$ ) of the samples were measured as a function of DC bias voltage ( $V$ ), and donor density ( $N_d$ ) was determined from the slope of  $(1/C - 1/2C_0)^2$  versus  $V$  graph drawn by  $(1/C_{gb} - 1/2C_{gb, (U=0)})^2 = 2(\Phi_{B0} + qU) / q^2 \epsilon N_d$ , [2] where  $\Phi_{B0}$  is the barrier height  $\Phi_B$  under zero bias,  $q$  is the charge of the electron,  $U$  is the individual voltage drop applied to the grain boundary,  $\epsilon$  and  $N_d$  are the dielectric constant and the donor density of ZnO, respectively. The density of interface states ( $N_t$ ) at the grain boundary is determined by the equation  $N_t = (2\epsilon N_d \Phi_B / q)^{1/2}$ . And the depletion layer width ( $L$ ) of either side at the grain boundaries is determined by the equation  $N_d L = N_t$ .

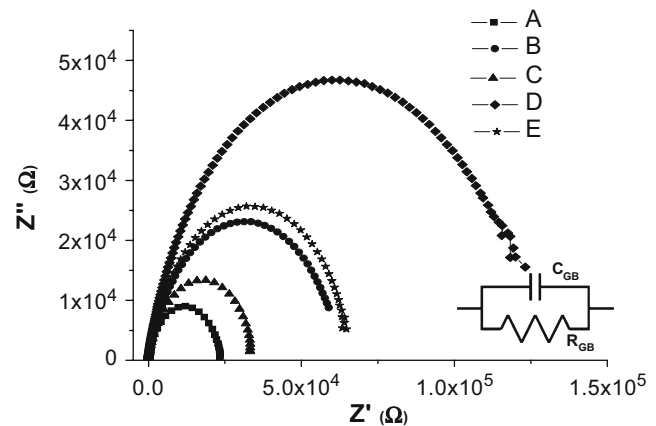


**Fig. 4** Impedance data for A to E at 190 °C with its equivalent circuit

**Table 1** The microstructure,  $V$ – $I$ ,  $C$ – $V$ , and complex resistance characteristic parameters of A to E pellets.

Sample	$d$ ( $\mu\text{m}$ )	$\rho$ ( $\text{g}\cdot\text{cm}^{-3}$ )	$V_{1\text{mA}}$ ( $\text{V}\cdot\text{mm}^{-1}$ )	$V_{\text{gb}}$ ( $\text{V}/\text{gb}$ )	$\alpha$	$N_{\text{d}}$ ( $10^{18}\text{cm}^{-3}$ )	$N_{\text{t}}$ ( $10^{12}\text{cm}^{-2}$ )	$\Phi_{\text{b}}$ (eV)	$L$ (nm)	$R_{\text{gb}}$ ( $10^4 \Omega$ at 190 °C)	$R_{\text{g}}$ ( $\Omega$ )
A	11.8	5.12	281	3.3	35.3	4.09	6.77	1.19	16.5	2.4	6.2
B	8.8	5.44	458	4.0	70.8	3.37	5.93	1.11	17.6	6.2	3.9
C	8.5	5.53	385	3.3	68.2	5.43	8.98	1.58	16.5	3.0	3.0
D	7.9	5.45	520	4.1	79.4	3.62	7.94	3.21	21.9	12.5	2.1
E	7.1	5.48	488	3.5	88.3	1.88	15.87	3.57	19.8	6.0	4.6

### 3 Results and discussion

Figure 1(a,b) shows the SEM micrographs for the ZnO powder that was subjected to 0 h and 12 h activation, respectively. There are some soft agglomerates after 12 h activation. However, it is obvious that the powder is greatly refined both in size and shape. For ZnO precursor, the BET specific area sharply increased from 2.94 to 6.65  $\text{m}^2/\text{g}$  after 6 h activation and then increased to 8.81  $\text{m}^2/\text{g}$  in slower rate after 12 h. Accordingly, the particle size of ZnO precursor calculated on the basis of specific surface area are 360, 184 and 120 nm for 0, 6 and 12 h activation. Additive size also decreased from 806 to 280 nm. The SEM photos are in good accordance with the BET specific surface area results. When mixed by a combination, particle sizes of A to E powders are understandably dependent on the size of ZnO powder as it occupies more than 90 wt% in the whole precursor. Additionally, the refined powder has acceleration in the densification due to the sintering activity gained from the high-energy activation, so it is reasonable to lower the sintering temperature.

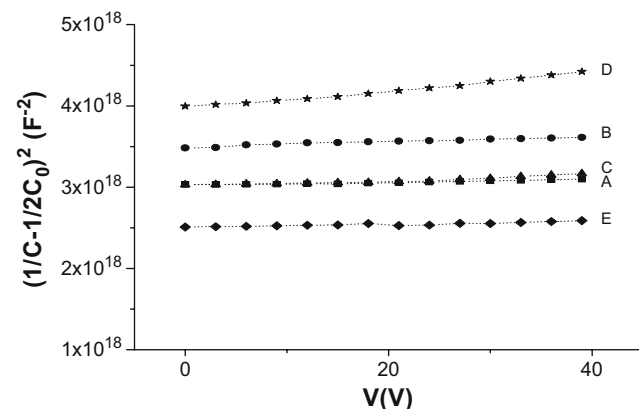


**Fig. 5** Voltage dependence of the contact capacitance  $C$  of the pellets sintered at 1140 °C with 100 kHz 1 mv amplitude ac voltage superimposing on dc bias from 0 to 40 V

In Fig. 2, we see the polished and thermally etched disk surface sintered at 1140 °C for 2 h. It is clear that sample A has a bigger average grain size up to 11.8  $\mu\text{m}$ , while the others contain smaller (ranging from 7–9  $\mu\text{m}$ ) and more homogeneous grains which give rise to the homogeneity in both the grain boundary and the triangle junctions [3] in between every three grains. This shows that the activation resulted in an effective refinement in the average grain size.

The current–voltage characteristics of the samples from A to E are presented in Fig. 3. Assuming that the voltage drop at each grain remains the same, it is understandable that break down voltage largely increases in the pellets prepared from the mechanically activated precursors due to the growing number of grains. When the grain size is approximately the same in sample B to E, the boundary junctions exhibit a continuous distribution of the break-down voltage  $V_{\text{b}}$ , the shape of the overall  $I$ – $V$  characteristic is sensitive to the deviation in grain boundary.

Grain and grain boundary resistance are obtained from the impedance data shown in Fig. 4. Their values are given in Table 1. For sample A, inhomogeneity is dominant in determining the easiest current paths [3]. In the relatively homogeneous grain boundary such as in pellet D, grain boundary's resistance sharply increases one magnitude

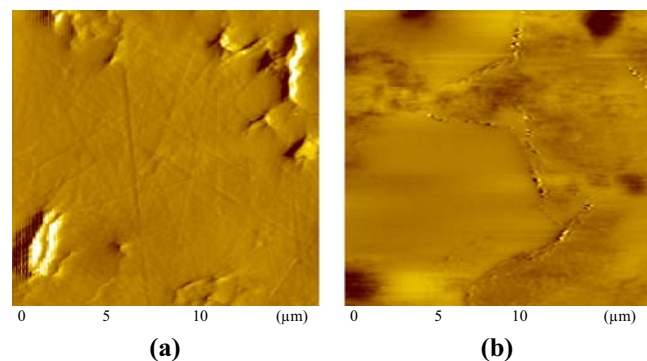


**Fig. 6** SS-PM image of Sample A (a) Topograph (b) Potential in plan view

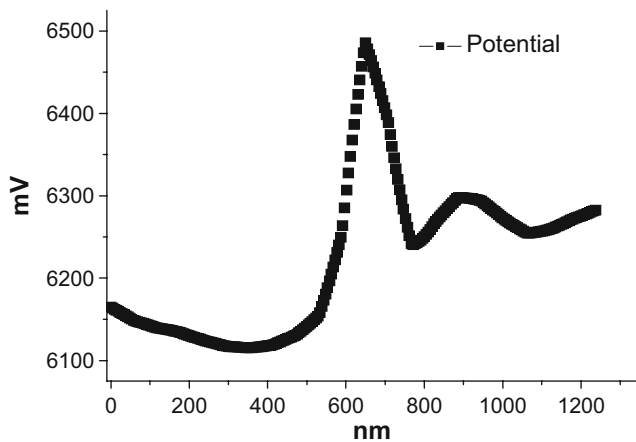


Fig. 7 Cross-section of potential line intercepted in grain boundary

higher. While the decrement in  $R_{gb}$  between B and C, or D and E can also be explained as the falling of dopants' amount per grain boundary. The voltage drop across a Schottky barrier is not the same thing as the Schottky barrier height, so it may be coincidence that two values are nearly equal in these varistor materials [4].

Figure 5 shows a C–V curve through which we obtained the value of  $\Phi_b$  (barrier height),  $N_d$  (donor density),  $N_t$  (interface state density) and  $L$  (depletion layer width), and their values are listed in Table 1. The increasing barrier height  $\Phi_b$  is the consequence of high-energy mechanical activation which makes more segregation of adsorbed impurity ions and crystalline elements such as Sb, Co in triangle junction and more homogeneous boundaries covered with rich Bismuth, where there is more chemical potential and energy distribution of grain-boundary states above the zero-bias Fermi level. Pike et al. [5] gave an empirical equation as  $\alpha = 0.46\Phi_{B0}/kT[1 - 0.013\ln(e^3N_t^2/4\epsilon\epsilon_0N_d)]$ , dependence of  $\alpha$  on  $N_d$  is very weak, while the variation of this quantity with temperature is substantial. It is easy to see from the equation that  $\alpha$  largely depends on the  $\Phi_{B0}$ , while  $\Phi_{B0}$  is greatly improved by high-energy activation. Therefore, the  $\alpha$  value increases with the increase of activation time.

The depletion layer width is found to be larger which results in the increase of the density of interface. To give a further evidence to support the data obtained in the work, a Scanning Surface Potential Microscope (SSPM) [6] is introduced. Figure 6(b) is the potential graph in accordance with the topography image (a). The grain size is read to be

approximately 10  $\mu\text{m}$  which is in close agreement with the result in Fig. 2.

The height of the potential is 479 mV from top to bottom within 15  $\mu\text{m}$  range in horizontal, the black regions in potential view is possibly Bi and Sb rich second phases. The asymmetry Schottky barrier height shown in Fig. 7 is 275 mV with grain boundary half width in 100 nm. The mismatching was due to the lift height which was determined as  $\Phi_z = \Phi_0 \exp(Bz^C)$  [6], where  $\Phi_z$  is the potential measured at certain height  $z$ ,  $\Phi_0$  is the potential at the interface,  $B$ , and  $C$  are constants.  $B$  and  $C$  equal  $-0.47 \pm 0.01$  and  $0.345 \pm 0.005$  [6], respectively. Using the functional form to determine the interface potential from the measurements yields  $1,890 \text{ mV} \pm 150$ , in good agreement with macroscopic measurements.

## 4 Conclusions

More homogeneous microstructure of ZnO varistor is achieved by introducing precursors prepared from high-energy mechanical activation (ball milling). A combination of precursors (ZnO and additive powders) is subjected to different activation time and their sintered body are studied which indicates an improvement in breakdown voltage and nonlinear coefficient  $\alpha$  value. These results correlated with the increase of Schottky barrier height and decrement of donor density.

**Acknowledgement** Financial support by the National Science Foundation NO. 50577065 and plan of the Shanghai Municipal Science and Technology Commission, 04DZ11603(2004–2006) are gratefully acknowledged.

## References

1. C.P. Fah, J. Wang, *Solid State Ion.* **132**, 107–117 (2000)
2. K. Mukae, K. Tsuda, I. Nagasawa, *J. Appl. Phys.* **50**, 4475–4476 (1977)
3. F.A. Modine, L.A. Boatner, in *Dielectric Ceramic Material: Influence of Ceramic Microstructure on varistor electrical properties*, ed. by K.M. Nair, A.S. Bhalla (The American Ceramic Society, Westerville, OH, 1999), p. 474
4. W.G. Morris, *J. Vac. Sci. Technol.* **13**(4), 926–931(1976)
5. G.E. Pike, C.H. Seager, *J. Appl. Phys.* **50**, 5 (1979)
6. B.D. Huey, D.A. Bonnel, *Solid State* **131**, 51–60 (2000)